LiNi_{1/3}Mn_{1/3}Co_{1/3}O₂,

Lithium Metal Battery Pouch Cell Assembly and Prototype Demonstration Using Tailored Polypropylene Separator

Manikandan Palanisamy, Vihang P. Parikh, Mihit H. Parekh, and Vilas G. Pol*

The development of realistic lithium metal batteries (LMBs) is highly desirable to address the steady increase in the energy-storage demand for high-power applications. Consequently, the polydopamine-tailored polypropylene separator enables scale up with \approx 8 μ m-thick graphene nanosheets coating on the polypropylene separator. A layered LiNi_{1/3}Mn_{1/3}Co_{1/3}O₂ (LNMC) cathode is characterized by X-ray diffraction analysis (XRD) and scanning electron microscopy (SEM) analysis, which exhibits single phase purity with a hexagonal structure, R3m space group, and a homogenized spherical shape morphology with secondary particles comprising primary particles. Lithium metal battery pouch cells (LMBPCs) are fabricated based on the proposed design strategies, containing a lithium metal anode, LNMC cathode, and tailored polypropylene separator without any internal short circuit, wherein polydopamine and graphene nanosheets layers are positioned toward the LNMC cathode in the pouch cell stacking order. The assembled pouch cell is cycled between 3.0 and 4.2 V and delivers a cell capacity of \approx 500 mAh. Then the charged LMBPCs are connected to the prototype electronic truck and demonstrated on various surfaces at 25 °C and < -5 °C. From the prototype truck demonstration results, LMBPCs are useful for practical high-power applications, including electric vehicles, hybrid electric vehicles, and grid energy storage.

1. Introduction

The 2019 Chemistry Nobel Prize-winning lithium-ion battery (LIB) technology is a highly promising energy source for the ever-growing energy demands compared with other rechargeable batteries. Consequently, the present LIBs have been successfully incorporated into portable consumer electronic devices, electric vehicles (EVs), and defense applications. In LIBs, different types of carbon (graphite, amorphous/hard carbon, porous carbons), alloys matrix (containing Si, Sn, Sb, Ni, Ti metals), composite alloys (a combination of carbon and an alloy), and metal oxides (Li₄Ti₅O₁₂, TiO₂, TiO₂, SnO₂, SnO₂, SnO₂, SnO₂, SnO₂, TiO₃) have been extensively studied in the past three decades as anode materials. The developed anodes have been combined with high-voltage cathodes, mainly LiCoO₂,

Dr. M. Palanisamy, V. P. Parikh, M. H. Parekh, Prof. V. G. Pol Davidson School of Chemical Engineering Purdue University West Lafayette, IN 47907, USA E-mail: vpol@purdue.edu

The ORCID identification number(s) for the author(s) of this article can be found under https://doi.org/10.1002/ente.202000094.

DOI: 10.1002/ente.202000094

materials, [21] demonstrating a prolonged cycling stability while maintaining a high Coulombic efficiency during chargedischarge cycles.^[2,3] However, the anode possesses intrinsic limitations such as solid-electrolyte interface (SEI) formation and its stability at a high rate for use in high-power applications, viz., EVs, hybrid electric vehicles (HEVs), and grid energy storage.[1-3] Indeed, there is a concern in LIBs with an electrode mass balance between the anode and cathode in terms of specific capacities and their formation cycle process carried out at a low current density. [22-24] During formation cycles, Li⁺ loss occurs due to the formation of SEI as a passivation film on an anode surface, consumed from the cathode source and simultaneous electrolytic decomposition reactions, leading to an overall reduced full cell capacity. [25–27] Furthermore, the SEI layer is limited to operate at a high cell voltage and leads to unexpected cell failure due to SEI damage by overcharge/ discharge

(LNMC), [19] LiMn₂O₄, [20] and LiMn₁ 5Ni₀ 5O₄

or at a high current density. Therefore, to address these anode intrinsic limitations, research and developments are required to focus on high-energy lithium metal batteries (LMBs) as superior rechargeable systems.

LiFePO₄,^[17,18]

LMB is the most promising next-generation technology with the highest theoretical capacity of lithium metal (3862 mAh g^{-1}), an utmost negative redox potential (-3.04 V vs standard hydrogen electrode), and a very low density $(0.53 \,\mathrm{g\,cm^{-3}})$. These properties enable their use in high-energy Li-S and Li-O₂ batteries.^[28–30] These exceptional properties can be translated to 300–500 Wh kg⁻¹ energy density and cost less than 100 USD (kWh)⁻¹, combined with the high-capacity cathode in pouch cell configuration. [31] Nevertheless, LMBs still face many challenges during cycling such as poor capacity retention and lithium dendritic growth. The latter leads to safety risk, eventually hindering their use in the consumer battery market.^[32,33] To address these issues, different strategies have been explored to attain a higher Coulombic efficiency and reduce the risk of short circuit. Particularly, the approaches of solid-state nanoscale film protection on the lithium metal surface, [34,35] electrolyte additive-derived films, $^{[36]}$ atomic layer-deposited protection layers, $^{[37]}$ chemical reaction-derived surface films, $^{[38,39]}$ lithium fluoride protection layers, [40] new electrolytes, [41] and a thin 3D structured lithium metal anode containing carbon host or porous

Cu or porous polymer membranes^[42–45] have been investigated. In contrast to these studies, the surface-tailored polypropylene separator modified with polydopamine and graphene, which is developed by our Purdue group, exhibited remarkable stability compared with a pristine polypropylene separator and exhibits 93% capacity retention after 1000 cycles.^[46] Therefore, the feasibility of assembly and prototype demonstration of LMBs are highly anticipated for the actual development of LMBPC.

With this perspective, the LMBs needs to be explored in pouch cell configuration for their utilization in EVs application with the design of large-scale geometry. Although stable and prolonged cycle life are achieved in LMBs, most of the reports are studied for coin cell configuration only.^[34–45] As the actual pouch cell performance is different from the coin cell results, in terms of energy density and cycle life, it can result in knowledge gaps while connecting the dots for real-life applications. To address the practical challenges of pouch cell performance, few studies have been reported with LMBPCs. [41,47] Nevertheless, the pouch cell performance has not been as promising as coin cell performance. Certainly, the pouch cell capacity is much greater than the coin-type cell and hence, minor defects arising in pouch cell components are integrated in the pouch cell performance, which leads to unidentifiable problems and reduced cell performance. [41,45,47] Thus, the actual cell capacity, total cell weight, cost, cell transport stability, and safety are needed to address the practical use of LMBs. [41,48,49] In this context, the pouch cell design strategies are essential factors to incorporate proposed new materials and concepts toward the further development of practical use of LMBs.

Herein, we assembled lithium metal battery pouch cells (LMBPCs) using polydopamine/graphene nanosheets-tailored polypropylene separator with lithium metal anode and LNMC cathode. Subsequently, the fabricated LMBPCs were subjected to charge–discharge cycles at an applied current of 50/100 mA and delivered a cell capacity of 500 mAh. Ultimately, the LMBPCs were connected in the prototype device, demonstrating an electronic truck and operating on two different surfaces at 25 °C and <-5 °C to implement the possible practical use of LMBs for EV application.

2. Results and Discussions

Due to concern regarding the steadily increasing energy demands, the development of high-energy LMBPCs is required for use in real-life applications. Nevertheless, it suffers from the key limitation of lithium dendritic growth, which leads to safety risk in real-life applications. Hence, to address these challenging issues, the tailored polypropylene separator is scaled up, as shown in **Figure 1**, with a consistent graphene layer thickness of $8 \, \mu m$.

2.1. Tailored Polypropylene Separator Scaled Up for Pouch Cell Fabrication

To implement LMBs in EV applications, research studies have been devoted to address the issue of low Coulombic efficiency and safety risk by lithium dendrite growth, wherein lithium

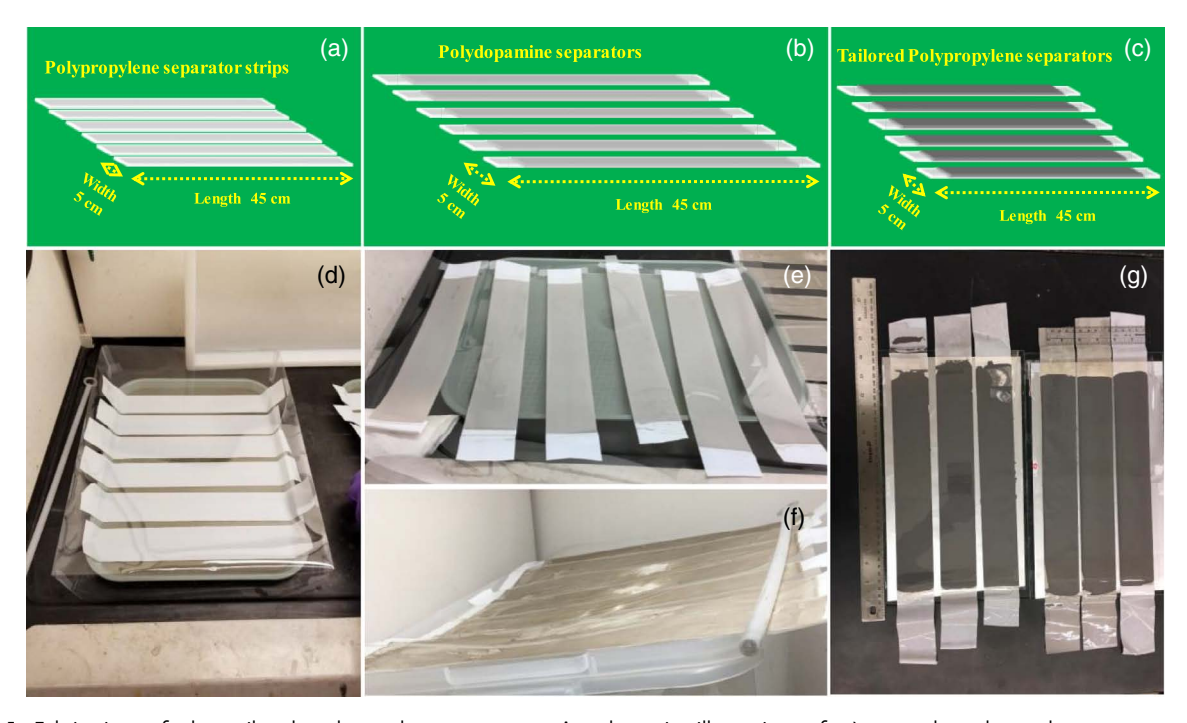


Figure 1. Fabrication of the tailored polypropylene separator. A schematic illustration of a) as-such polypropylene separator strips, b) polydopamine surface-treated separator, c) tailored polypropylene separator, and d) actual Celgard polypropylene separator floated onto the dopamine solution; e,f) after drying the surface-treated polypropylene separator appeared slightly brown; g) obtained tailored polypropylene separator by casting the homogenized slurry of graphene nanosheet powder and carboxymethyl cellulose binder in water, onto the surface-altered polydopamine separator.

metal is used as an anode. The conventional Celgard polypropylene separator exhibits a hydrophobic behavior with electrolyte and leads to poor electrochemical kinetics; particularly, the cell performance decreases at a high current density (>1 mA cm⁻²) applied to LMBs. [41,50] Hence, the surface of the polypropylene separator is functionalized by dopamine and polymerized to polydopamine, which enables hydrophilicity to polypropylene for electrolyte and enhances wettability. [51,52] Further, graphene nanosheets [53–55] with a carboxymethyl cellulose binder were coated on the polydopamine layer, which achieved improved lithium storage and specific capacity in Li versus the LiFePO₄ cell over 1000 cycles. This can be attributed to the additional conductive path through graphene nanosheets and mitigating electrode volume changes during the cycling process, as we reported in our earlier study. [46]

To provide further insights on the characteristics of the tailored polypropylene separator, [46] studies are extended to LMBPC assembly (Li vs LNMC) and prototype truck demonstration for practical use of LMBs in EV applications. Accordingly, the tailored polypropylene separator process was integrated to the required quantities of LMBPCs, as shown in Figure 1a–c. In this context, the Celgard polypropylene separator floated on the dopamine solution for 2 h, containing methanol and tris-buffer solution (pH of 8.5), as shown in Figure 1d.

Notably, after drying, the surface-treated polydopamine separator appeared slightly brown, as shown in Figure 1e,f. Consequently, the homogenized slurry, containing 90% graphene nanosheets powder and 10% carboxymethyl cellulose binder, was casted onto the surface-altered polydopamine separator and dried in a vacuum oven at 50 °C for 24 h (Figure 1g). The tailored polypropylene separators were stored inside the glovebox with a size of $5.0 \times 5.5 \, \mathrm{cm}^2$ to fabricate lithium metal pouch cells and subjected to further scanning electron microscopic analysis.

The surface morphologies and coating thickness of polypropylene, polydopamine, and the tailored polypropylene separator were investigated using the scanning electron microscopy (SEM) technique, as shown in **Figure 2**. The polypropylene separator has plenty of pores (Figure 2a,b), with a thickness of $\approx\!25\,\mu\text{m}$, as shown in Figure 2c,d, corroborated with the literature report. Then the surface-treated polydopamine separator was completely covered with the polydopamine layer (Figure 2e–h) and appeared slightly brown (Figure 1e,f). Remarkably, most of the pores of the polypropylene separator were filled by polydopamine without any volume changes (Figure 2g,h), related to the pristine polypropylene separator, as shown clearly in Figure 2a,b and Figure 2e,f. Further, the modified polypropylene separator revealed a flakey morphology (Figure 2i,j) corresponding to the presence of graphene

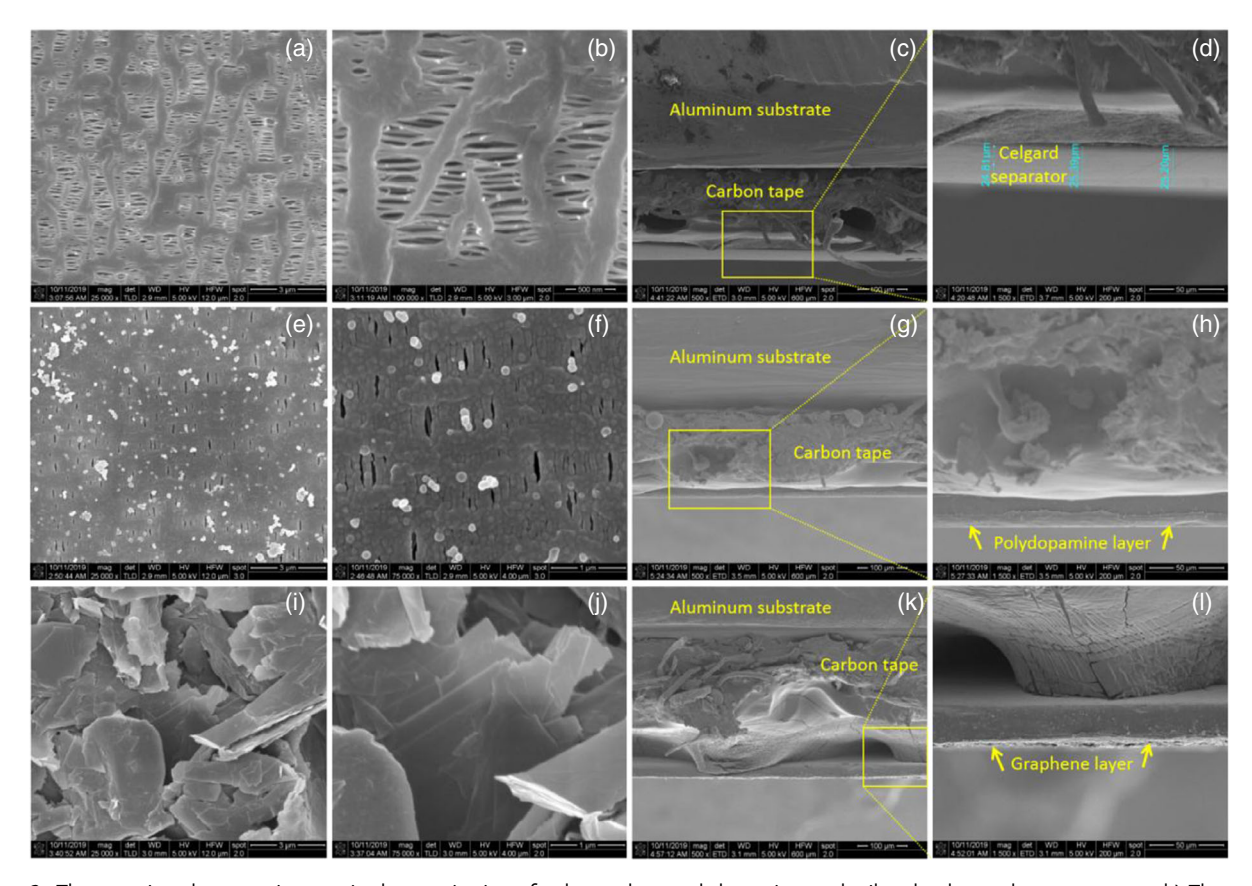


Figure 2. The scanning electron microscopic characterization of polypropylene, polydopamine, and tailored polypropylene separator: a,b) The surface morphology of polypropylene separator; c,d) thickness measured by cross-section images for polypropylene separator; e,f) surface morphology of polydopamine layer, coated on one side of the polypropylene separator; g,h) polydopamine coating layer indicated on the polypropylene separator; i,j) tailored polypropylene separator revealing flakey morphology corresponding to the presence of graphene nanosheets; and k,l) investigation of graphene layer thickness in the tailored polypropylene separator.

nanosheets morphology [57,58] with a coating layer thickness of $\approx\!\!8\,\mu m$, as shown in Figure 2k,l. Obviously, graphene nanosheets with a size of $\approx\!\!2\,\mu m$ were well dispersed on the polydopamine layer with a uniform layer coating, as shown in Figure 2l. From the consistent results, we report that the tailored polypropylene separator is developed in a laboratory setup at a large scale for LMBPCs.

2.2. Structural Characterization of LNMC Cathode Material

To describe the cathode physical properties, the powder was collected from the actual cathode, containing LNMC material, super carbon, and PVdF binder, and examined by a powder X-ray diffraction analysis (XRD) pattern, as shown in Figure S1a, Supporting Information. It is shown that all the diffraction peaks (blue) were well indexed with LNMC material related to the standard diffraction pattern ICPDS# 01-087-1564 (red). adopting $R\bar{3}m$ space group and a hexagonal α -NaFeO₂-type structure. [19,59,60] From the obtained XRD results, it is confirmed that no other impurity or a different phase is present along the LNMC cathode. Further, the morphology and particle size for collected materials were investigated by the scanning electron microscopic technique, as shown in Figure S1b-e, Supporting Information. Significantly, the LNMC cathode material exhibited a homogenized spherical shape morphology, corresponding to the presence of secondary particles with a size of 10 µm, formed by the agglomeration of primary particles (1 µm), as shown in Figure S1e, Supporting Information. The presence of primary and secondary particle morphologies were corroborated with the literature reports. [61,62] Also, an elemental mapping (Figure S2a-h, Supporting Information) and energy-dispersive X-ray (EDX) spectrum (Figure S2i, Supporting Information) of the collected cathode material showed the presence of Ni (green), Mn (cyan), Co (red), O (yellow), C (light green), and F (purple) elements, wherein the Li signal did not appear due to an EDX

analysis limitation. Notably, the presence of C (light green) and F (purple) were associated with the existence of super carbon and PVdF binder in the cathode, as shown in Figure S2g and S2h, Supporting Information.

2.3. Schematic Illustration of LMBPCs

To address the steadily increasing energy demands, highenergy-density LMBs have been devoted with the new materials and concepts. [28,29] Accordingly, most of the approaches were well defined to overcome the issues of lithium dendritic growth and safety risks under coin cell configurations.[34-45] From the literatures, [41,45,47] LMB performance in the coin cell configuration is quite different corresponding to the actual highenergy-density LMBPC for use in high-power applications. Hence, in this report on the modified polypropylene separator, the study^[46] further extended LMBPC assembly and prototype demonstration, wherein the lithium metal foil (indicated in light gray, size $4.5 \times 5.0 \,\mathrm{cm}^2$) was placed on the Cu current collector (orange) based on the required single-side (two) and double-side anodes (three), as shown in Figure 3. Subsequently, similar sizes of four double-side-coated cathodes containing LNMC, super carbon, PVdF binder, and the fabricated tailored polypropylene separator (indicated with polypropylene in blue, polydopamine in pink, and graphene in green) were used to assemble LMBPC, as shown in Figure 3. Subsequently, LMBPC was assembled by the sealing of an aluminum pouch cover with lithium metal anode, LNMC cathode, and tailored polypropylene separators stacked together, having a typical multilayer structure, as shown in Figure 3. Importantly, the polydopamine and graphene nanosheets layers (coated on polypropylene) were positioned toward the LNMC cathode in the pouch cell stack. Remarkably, we described here the pouch cell design strategies for practical use of LMBs using tailored polypropylene separator.

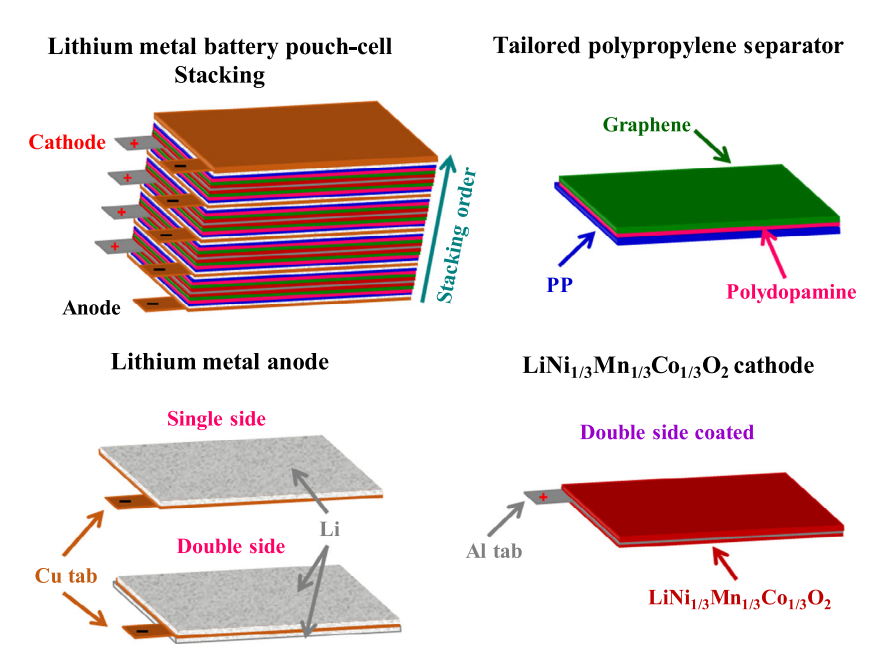


Figure 3. LMBPC: Schematic illustration for the LMBPC stacking order using lithium metal anode, tailored polypropylene separator, and LNMC cathode.

2.4. Charge—Discharge Cycling Performance of LMBPCs and Prototype Truck Demonstration

According to our proposed design strategies, LMBPCs were fabricated using lithium metal anode, LNMC cathode, and tailored polypropylene separator for the reasons of light weight, low cost, and a high energy density over other types. [63] The measured open-circuit voltage of the assembled pouch cell was 3.02 V, as shown in the inset (#) of Figure 4a. For practical use of the prototype demonstration, the initial cycle was carried out at 50 mA between 3.0 and 4.2 V and then increased to 100 mA. From the cell voltage versus time and current versus time plots, the fabricated pouch cell was enabled to charge/discharge for \approx 10 h (at 50 mA) and \approx 4 h (at 100 mA), corresponding to the first and 2-5 cycles, as shown in Figure 4a. Notably, the plot of cell voltage versus cell capacity profile shows slope voltage profiles and a delivered cell capacity of ≈500 mAh for the LNMC cathode, used in pouch cell fabrication (Figure 4b). The obtained slope voltage profile was corroborated with the pouch cell reports, [41,47] assembled with the LNMC cathode. Further, the cycling studies of LMBPC were limited to five cycles and used for the prototype demonstration of the electronic truck

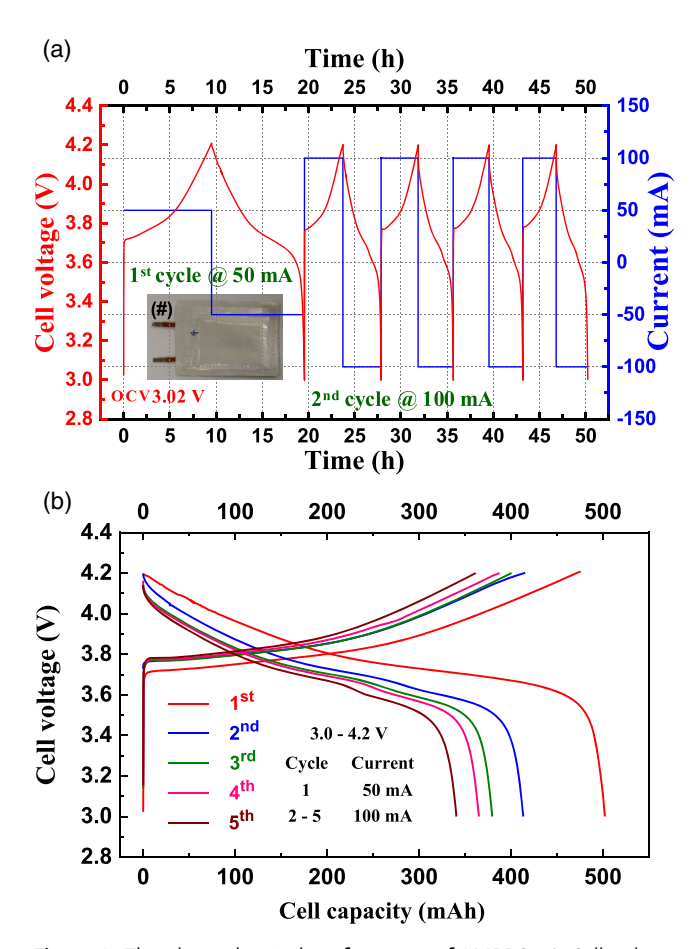


Figure 4. The electrochemical performance of LMBPC: a) Cell voltage versus time and current versus time plots for the fabricated pouch cell shown in inset (#) and b) cell voltage versus cell capacity profile associated with LNMC cathode used in pouch cell fabrication between 3.0 and 4.2 V at 50 and 100 mA, corresponding to first and 2–5 cycles.

(**Figure 5**a). Thus, the charged LMBPC was used to power electronic trucks on the floor and LEDs on Purdue University campus at 25 °C and < -5 °C, as shown in Figure 5b–e. In addition, the demonstrated video files of the electronic truck at 25 °C and < -5 °C are given in video files, Supporting Information (Demonstration–V1 25 °C and Demonstration–V2 -5 °C) to explore the practical use of LMBPC. From the prototype demonstration, LMBPCs assembled with the modified polypropylene separator are of interest in high-power applications, viz., EVs, HEVs, and grid energy storage.

2.5. Deliberations on the Challenging Issues of LMBPCs

As described in the literature reports, [41,45,47] to obtain the high performance of LMBPCs (similar to coin cells) for practical use is highly challenging and requires intensive research studies to address the key issues that affect the pouch cells' performance. Accordingly, from the charge-discharge cycles of LMBPCs (Figure 4), it is pertinent to note that a significant capacity fade was observed for LMBPCs, assembled with a tailored polypropylene separator. This capacity decay can be attributed to Li degradation and SEI buildup, as shown in literature reports. [32,33] To minimize the capacity fade during cycles, the critical parameters, viz., stack pressure, uniform wettability of electrodes, cathode mass loading with respect to the lithium metal anode, and electrolyte filling, are needed to validate exactly for LMBPCs. [41,47] Further, carbonate-based 1 M LiPF₆ in the EC-DEC mixture solution was used as electrolyte in assembled pouch cells, which could be one of the principal reasons for capacity fade. The carbonate electrolyte is not compatible with lithium metal anode, especially in the pouch cell design, as discussed in pioneering reports, whereas it is designed for graphite anodes used in LIBs. [64,65] Deliberately, lithium bis(fluorosulfonyl) imide with triethyl phosphate/bis(2,2,2-trifluoroethyl) ether was used as an alternative superior electrolyte instead of carbonate electrolyte to enable prolonged cycles. This cutting-edge electrolyte certainly impedes lithium depletion and mitigates the unwanted chemical reaction between electrodes and electrolyte. [41] Importantly, LMBPCs are needed to be assembled in ultra-high vacuum with the least electrolyte to avoid pouch cell swelling and attain a uniform stack compactness. Ultimately, a conductive carbon cloth and 3D-designed porous Cu foam that support the ultrathin lithium metal^[42–45] are the most stable anodes for LMBs. Accordingly, all these appropriate approaches can be implemented along with the tailored polypropylene separator to overcome the anode's intrinsic limitations (a low Coulombic efficiency and dendritic lithium growth) and achieve a prolonged cycle stability for the next-generation LMBPCs to realize its practical use in EV applications.

3. Conclusions

Herein, we conclude that the tailored polypropylene separator enabled scaling up for the fabrication of LMBPCs. The surface morphology and the coating thickness of polypropylene, polydopamine, and tailored polypropylene separator were achieved with consistency for large-scale preparation, which was confirmed by SEM images. Remarkably, the modified polypropylene

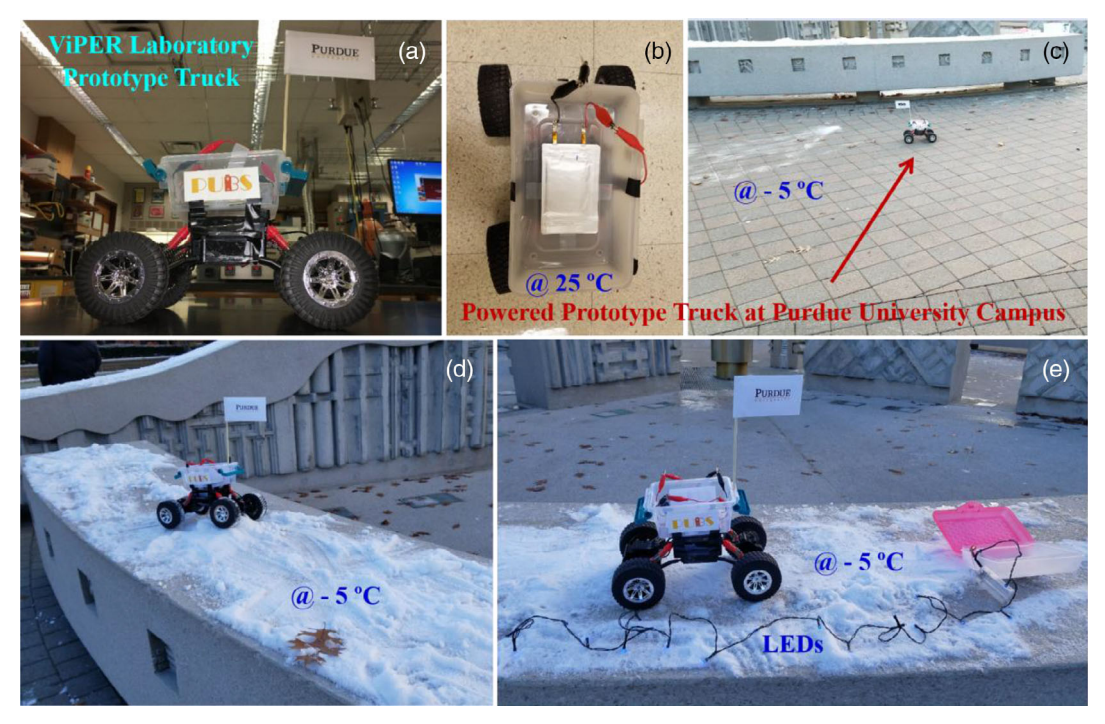


Figure 5. Prototype device of electronic truck demonstration: a) Prototype device of electronic truck; charged LMBPC powered to electronic truck at Purdue University campus b) at 25 °C, c,d) < -5 °C, and e) LEDs at < -5 °C to explore on the practical use of LMBPC.

separator exhibited graphene nanosheets morphology with a coating layer thickness of $\approx 8 \, \mu \text{m}$ on the polypropylene separator (thickness of $\approx 25 \,\mu\text{m}$). To implement the developed modified separator in actual LMBPCs, lithium metal anodes were fabricated using a lithium metal foil and LNMC cathode. The XRD and SEM of cathodes revealed a hexagonal structure with $R\bar{3}m$ space group and a homogenized spherical shape morphology for the presence of primary and secondary particles. Then, as per our proposed pouch cell design strategy, the LMBPCs were assembled using the lithium metal anode, LNMC cathode, and a tailored polypropylene separator. Thus, the fabricated pouch cells were cycled between 3.0 and 4.2 V and delivered a cell capacity of \approx 500 mAh. After five cycles, the charged LMBPC was connected in the prototype truck and powered to operate on different surfaces in Purdue University campus at 25 °C and < -5 °C to explore its practical use with the tailored polypropylene separator. Finally, the obtained capacity fade during pouch cell cycling was discussed in detail regarding the challenging issues for the next-generation LMBPCs. From the obtained result of the prototype electronic truck demonstration on various surfaces at 25 °C and < -5 °C and the deliberations on the challenging issues for LMBPCs, the development of LMBPCs for prolong cycling stability holds a solid vision for EVs, HEVs, and highenergy grid storage applications.

4. Experimental Section

The assembly of the lithium metal pouch cell consisted of three steps:

1) the preparation of the tailored polypropylene separator using polydopamine and graphene nanosheets with carboxymethyl cellulose binder,

2) the fabrication of electrodes (lithium metal anode and NMC cathode), and 3) pouch cell stacking using anode, cathode, and tailored polypropylene separator.

Preparation of Tailored Polypropylene Separator and Characterization: The process of modifying the separators starts with floating the polypropylene separator strips (Celgard 2500) on dopamine solution (10×10^{-3} M) containing methanol and tris-buffer solvents with pH 8.5 for 2 h. Then, the separator treated with polydopamine was dried in an oven at 50 °C for 10 h and the surface-altered polypropylene separator was obtained. The homogenized aqueous slurry (using planetary Thinky mixer) containing 90% (wt) graphene nanosheets powder (Graphene Supermarket) and 10% (wt) carboxymethyl cellulose binder (Sigma Aldrich) with Millipore water was casted onto the polydopamine surface in the polypropylene separator and dried in vacuum oven at 50 °C for 24 h. Finally, the surface morphologies and coating thickness of polypropylene, polydopamine, and tailored polypropylene separators were examined using a scanning electron microscope (Nova nanoSEM 200). The well-characterized modifield polypropylene separator was cut with the size of $5.0 \times 5.5 \text{ cm}^2$ and used to fabricate LMBPCs.

Electrode Preparation and its Characterization: Lithium metal anodes were fabricated by gently hand pressing the lithium metal foil on $4.5 \times 5.0 \, \text{cm}^2$ -sized copper pieces. Two single-sided and three double-sided anodes were used per pouch cell. The cathode contained 90% (wt) LNMC, 5% super carbon, and 5% PVdF binder, which was cut into the size of $4.5 \times 5.0 \, \text{cm}^2$ (corresponding to the lithium metal anode). The phase purity and crystallinity of LNMC material in the cathode were analyzed by powder XRD analysis, recorded in the 2θ range between 10° and 80° using a Rigaku diffractometer with Cu Kα X-ray source. To determine the surface morphology and coating thickness of separators and particle size and the presence of elements of the LNMC cathode, SEM and elemental mapping with EDX analysis were examined using Nova nanoSEM 200 scanning electron microscope instruments and JEOL (JCM-6000PLUS, JED-2300 AnalysisStation).

LMBPC Assembly: While assembling LMBPCs, tailored polypropylene separators were positioned in such a way that the coated side faced toward

the LNMC cathode and was placed between each lithium metal anode and LNMC cathode interface. The number of stacked pairs of the anodecathode in a similar fashion was calculated based on the required pouch cell capacity. Further, the stacked electrodes were kept in an aluminum pouch and perfectly vacuum sealed while filling 1 $_{\rm M}$ LiPF $_{\rm 6}$ in EC–DEC (1:1, v/v) electrolyte. All assembly steps described earlier were conducted in an argon-filled glovebox (NEXUS II Vacuum Atmospheres Co.) with O2 and moisture levels controlled at <0.5 ppm. The fabricated LMBPCs were used for galvanostatic charge–discharge cycles between 3.0 and 4.2 V at 50/100 mA using Arbin cycler (Model BT2043) at 25 $^{\circ}$ C. After the cycling performance, the LMBPCs were connected in the prototype device and successfully powered the electronic truck running on the floor at 25 $^{\circ}$ C and $<-5^{\circ}$ C.

Supporting Information

Supporting Information is available from the Wiley Online Library or from the author.

Acknowledgements

The authors truly thank the financial support from the Office of Naval Research (grant no. N00014-18-1-2397). The LNMC cathodes were produced at the US Department of Energy's (DOE) CAMP (Cell Analysis, Modeling, and Prototyping) Facility, Argonne National Laboratory. The CAMP Facility is fully supported by the DOE Vehicle Technologies Program (VTP) within the core funding of the Applied Battery Research (ABR) for Transportation Program.

Conflict of Interest

The authors declare no conflict of interest.

Keywords

charge-discharge cycling, graphene nanosheets coatings, lithium metal battery pouch cells, prototype demonstrations, tailored polypropylene separators

Received: January 26, 2020 Revised: February 23, 2020 Published online: March 23, 2020

- [1] M. Armand, J. M. Tarascon, Nature 2008, 451, 652.
- [2] M. S. Whittingham, Chem. Rev. 2004, 104, 4271.
- [3] J. B. Goodenough, K. S. Park, J. Am. Chem. Soc. 2013, 135, 1167.
 [4] L. Zhang, M. Zhang, Y. Wang, Z. Zhang, G. Kan, C. Wang, Z. Zhong,
- F. Su, J. Mater. Chem. A **2014**, *2*, 10161.
 [5] T. P. Kumar, T. S. D. Kumari, A. M. Stephan, I. Indian Inst. Sci. **200**
- [5] T. P. Kumar, T. S. D. Kumari, A. M. Stephan, J. Indian Inst. Sci. 2009, 89, 394
- [6] L. S. Roselin, R. S. Juang, C. T. Hsieh, S. Sagadevan, A. Umar, R. Selvin, H. H. Hegazy, *Materials* 2019, 12, 1229.
- [7] S. H. Kim, D. H. Lee, C. Park, D. W. Kim, J. Power Sources 2018, 395, 328.
- [8] A. Ulus, Y. Rosenberg, L. Burstein, E. Peled, J. Electrochem. Soc. 2002, 149, A635.
- [9] W. J. Zhang, J. Power Sources 2011, 196, 13.
- [10] M. N. Obrovac, V. L. Chevrier, Chem. Rev. 2014, 114, 11444.
- [11] T. F. Yi, S. Y. Yang, Y. Xie, J. Mater. Chem. A 2015, 3, 5750.
- [12] K. Li, B. Li, J. Wu, F. Kang, J. K. Kim, T. Y. Zhang, ACS Appl. Mater. Interfaces 2017, 9, 35917.

- [13] S. M. Hwang, Y. G. Lim, J. G. Kim, Y. U. Heo, J. H. Lim, Y. Yamauchi, M. S. Park, Y. J. Kim, S. X. Dou, J. H. Kim, Nano Energy 2014, 10, 53.
- [14] H. Xue, J. Zhao, J. Tang, H. Gong, P. He, H. Zhou, Y. Yamauchi, J. He, Chem. Eur. J. 2016, 22, 4915.
- [15] J. Lee, J. Moon, S. A. Han, J. Kim, V. Malgras, Y. U. Heo, H. Kim, S. M. Lee, H. K. Liu, S. X. Dou, Y. Yamauchi, M. S. Park, J. H. Kim, ACS Nano 2019, 13, 9607.
- [16] K. Mizushima, P. C. Jones, P. J. Wiseman, J. B. Goodenough, *Mater. Res. Bull.* 1980, 15, 783.
- [17] A. K. Padhi, K. S. Nanjundaswamy, J. B. Goodenough, J. Electrochem. Soc. 1997, 144, 1188.
- [18] A. K. Pathi, K. S. Nanjundaswamy, C. Masquelier, S. Okada, J. B. Goodenough, J. Electrochem. Soc. 1997, 144, 1609.
- [19] T. Ohzuku, Y. Makimura, Chem. Lett. 2001, 30, 642.
- [20] M. M. Thackeray, P. J. Johnson, L. A. De Picciotto, P. G. Bruce, J. B. Goodenough, Mater. Res. Bull. 1984, 19, 179.
- [21] K. Amine, H. Tukamoto, H. Yasuda, Y. Fuiita, J. Electrochem. Soc. 1996, 143, 1607.
- [22] J. Kasnatscheew, T. Placke, B. Streipert, S. Rothermel, R. Wagner, P. Meister, I. C. Laskovic, M. Winter, J. Electrochem. Soc. 2017, 164, A2479.
- [23] M. Safari, C. Delacourt, J. Electrochem. Soc. 2011, 158, A1123.
- [24] J. Jiang, W. Shi, J. Zheng, P. Zuo, J. Xiao, X. Chen, W. Xu, J. G. Zhang, J. Electrochem. Soc. 2013, 161, A336.
- [25] E. Peled, J. Electrochem. Soc. 1979, 126, 2047.
- [26] P. Verma, P. Maire, P. Novak, Electrochim. Acta 2010, 55, 6332.
- [27] S. J. An, J. Li, C. Daniel, D. Mohanty, S. Nagpure, D. L. Wood, *Carbon* 2016, 105, 52.
- [28] W. Xu, J. Wang, F. Ding, X. Chen, E. Nasybulin, Y. Zhang, J. G. Zhang, Energy Environ. Sci. 2014, 7, 513.
- [29] D. Lin, Y. Liu, Y. Cui, Nat. Nanotechnol. 2017, 12, 194.
- [30] C. Yang, K. Fu, Y. Zhang, E. Hitz, L. Hu, Adv. Mater. 2017, 29, 1701169.
- [31] R. V. Noorden, Nature 2014, 507, 26.
- [32] J. M. Tarascon, M. Armand, Nature 2001, 414, 359.
- [33] J. B. Goodenough, Y. Kim, Chem. Mater. 2010, 22, 587.
- [34] Y. Li, Y. Sun, A. Pei, K. Chen, A. Vailionis, Y. Li, G. Zheng, J. Sun, Y. Cui, ACS Cent. Sci. 2018, 4, 97.
- [35] W. Li, H. Yao, K. Yan, G. Zheng, Z. Liang, Y. M. Chiang, Y. Cui, Nat. Commun. 2015, 6, 7436.
- [36] H. Ota, K. Shima, M. Ue, J. I. Yamaki, Electrochim. Acta 2004, 49, 565.
- [37] A. C. Kozen, C. F. Lin, A. J. Pearse, M. A. Schroeder, X. Han, L. Hu, S. B. Lee, G. W. Rubloff, M. Noked, ACS Nano 2015, 9, 5884.
- [38] X. Liang, Q. Pang, I. R. Kochetkov, M. S. Sempere, H. Huang, X. Sun, L. F. Nazar, *Nat. Energy* **2017**, *2*, 17119.
- [39] N. W. Li, Y. X. Yin, C. P. Yang, Y. G. Guo, Adv. Mater. 2016, 28, 1853.
- [40] D. Lin, Y. Liu, W. Chen, G. Zhou, K. Liu, B. Dunn, Y. Cui, Nano Lett. 2017, 17, 3731.
- [41] C. Niu, H. Lee, S. Chen, Q. Li, J. Du, W. Xu, J. G. Zhang, M. S. Whittingham, J. Xiao, J. Liu, Nat. Energy 2019, 4, 551.
- [42] Z. Liang, D. Lin, J. Zhao, Z. Lu, Y. Liu, C. Liu, Y. Lu, H. Wang, K. Yan, X. Tao, Y. Cui, Proc. Natl. Acad. Sci. 2016, 113, 2862.
- [43] H. Ye, S. Xin, Y. X. Yin, J. Y. Li, Y. G. Guo, L. J. Wan, J. Am. Chem. Soc. 2017, 139, 5916.
- [44] Y. Liu, Q. Liu, L. Xin, Y. Liu, F. Yang, E. A. Stach, J. Xie, Nat. Energy 2017, 2, 17083.
- [45] J. Liu, Z. Bao, Y. Cui, E. J. Dufek, J. B. Goodenough, P. Khalifah, Q. Li, B. Y. Liaw, P. Liu, A. Manthiram, Y. S. Meng, V. R. Subramanian, M. F. Toney, V. V. Viswanathan, M. S. Whittingham, J. Xiao, W. Xu, J. Yang, X. Q. Yang, J. G. Zhang, Nat. Energy 2019, 4, 180.
- [46] P. J. Kim, V. G. Pol, Adv. Energy Mater. 2018, 8, 1802665.
- [47] S. Chen, C. Niu, H. Lee, Q. Li, L. Yu, W. Xu, J. G. Zhang, J. G. Dufek, E. J. Whittingham, M. S. Meng, J. Xiao, *Joule* 2019, 3, 1094.

www.entechnol.de



www.advancedsciencenews.com

- [48] A. Kumar, S. Kalnaus, S. Simunovic, S. Gorti, S. Allu, J. A. Turner, J. Electrochem. Soc. 2016, 163, A2494.
- [49] T. Bond, J. Zhou, J. Cutler, J. Electrochem. Soc. 2016, 164, A6158.
- [50] J. Zheng, M. H. Engelhard, D. Mei, S. Jiao, B. J. Polzin, J. G. Zhang, W. Xu, Nat. Energy 2017, 2, 17012.
- [51] M. H. Ryou, D. J. Lee, J. N. Lee, Y. M. Lee, J. K. Park, J. W. Choi, Adv. Energy Mater. 2012, 2, 645.
- [52] M. H. Ryou, Y. M. Lee, J. K. Park, J. W. Choi, Adv. Mater. 2011, 23, 3066.
- [53] T. T. Zuo, X. W. Wu, C. P. Yang, Y. X. Yin, H. Ye, N. W. Li, Y. G. Guo, Adv. Mater. 2017, 29, 1700389.
- [54] C. P. Yang, Y. X. Yin, S. F. Zhang, N. W. Li, Y. G. Guo, Nat. Commun. **2015**, *6*, 8058.
- [55] Y. Zhang, B. Liu, E. Hitz, W. Luo, Y. Yao, Y. Li, J. Dai, C. Chen, Y. Wang, C. Yang, H. Li, L. Hu, Nano Res. 2017, 10, 1356.

- [56] B. Xiong, R. Chen, F. Zeng, J. Kang, Y. Men, J. Membr. Sci. 2018, 545, 213.
- [57] F. Pei, L. Lin, A. Fu, S. Mo, D. Ou, X. Fang, N. Zheng, *Joule* **2018**, 2, 323.
- [58] G. Wang, X. Shen, J. Yao, J. Park, Carbon 2009, 47, 2049.
- [59] Y. S. He, Z. Ma, X. Z. Liao, Y. Jiang, J. Power Sources 2007, 163, 1053.
- [60] F. Wu, M. Wang, Y. Su, L. Bao, S. Chen, J. Power Sources 2010, 195, 2362.
- [61] X. Luo, X. Wang, L. Liao, S. Gamboa, P. J. Sebastian, J. Power Sources 2006, 158, 654.
- [62] C. Julien, A. Mauger, K. Zaghib, H. Groult, Materials 2016, 9, 595.
- [63] K. Amine, I. Belharouak, Z. Chen, T. Tran, H. Yumoto, N. Ota, S. T. Myung, Y. K. Sun, Adv. Mater. 2010, 22, 3052.
- [64] B. Wu, J. Lochala, T. Taverne, J. Xiao, Nano Energy 2017, 40, 34.
- [65] J. Yu, N. Gao, J. Peng, N. Ma, X. Liu, C. Shen, K. Xie, Z. Fang, Front. Chem. 2019, 7, 494.